

NOISE ANALYSIS FOR DIFFRACTION ENHANCED IMAGING*

Jovan G. Brankov, Alejandro Sáiz-Herranz, and Miles N. Wernick

Department of Electrical and Computer Engineering,
Illinois Institute of Technology, Chicago, IL 60616, USA

ABSTRACT

Herein we present a quantitative noise analysis of diffraction enhanced imaging (DEI), an x-ray imaging method that produces absorption and refraction images, with inherent immunity to wide-angle scatter. DEI produces remarkable images, but requires an x-ray source of very high power; therefore, it has principally been confined to synchrotron studies. Clinical systems currently under development using conventional x-ray sources will be photon-limited. Therefore, it is important that the noise properties of DEI be understood. Herein, we show that the original formulation of DEI, given by Chapman, *et al* [1], is the maximum-likelihood solution of the image-estimation problem for the case of Poisson noise. We derive the mean, covariance and signal-to-noise ratio of the images produced by this method, which sheds light on the effect of system parameters on the computed images. We will use these results in future work to derive reconstruction methods that are more optimal in the presence of noise than the original DEI formulation.

1. INTRODUCTION

Diffraction enhanced imaging (DEI) [1] is a phase-sensitive imaging technique which can extract object properties in the form of refraction and apparent absorption images. Furthermore, DEI exploits wide angle scatter rejection contrast to provide images that have been shown to improve dramatically the visibility of small, low-absorbing structures as compared to conventional radiography [2-5].

A typical DEI set-up is represented in Figure 1. In DEI, a monochromated x-ray beam is passed through the object, then the angular composition of the beam analyzed by a perfect crystal. The high angular selectivity of the crystal allows tiny beam deflections caused by refraction to be detected. The DEI refraction image has been shown to be well suited for morphological studies of soft tissues [3,4]. Both the absorption and refraction images produced by DEI are superior to conventional radiographs due to the scatter rejection provided by the crystal system [3].

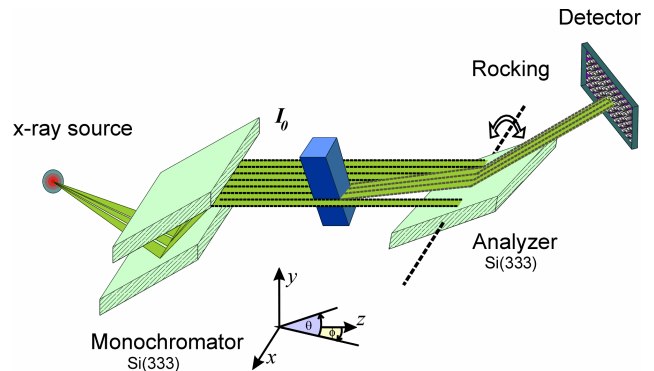


Fig. 1 Typical DEI setup. The beam is monochromated before hitting the object and the analyzer crystal is rotated (rocked) to analyze transmitted beam angular components.

A clinical version of the DEI system is being developed at our institution. Owing to the amount of light lost by the monochromator, a clinical system based on a conventional x-ray source will likely be photon-limited. Therefore, it is important that we understand the behavior of DEI in the presence of Poisson noise. The aim of this paper is to provide a basic understanding of DEI noise properties to aid in the development and evaluation of DEI systems and reconstruction algorithms. To the best of our knowledge, such an analysis has not before been performed, probably due to the fact that synchrotron sources are extremely bright, resulting in images that are essentially noise-free as compared with most clinical medical-imaging modalities.

2. DEI ESTIMATOR

The x-ray intensity, after traversing an object, can be described by Beer's law:

$$I_R(x, y) \cong I_0 \exp\left(-\int \mu(x, y, z) dz\right), \quad (1)$$

where I_0 represents the incident beam intensity and $\mu(x, y, z)$ describes the object's apparent absorption (extinction) coefficient.

The direction of the emerging beam is altered by refraction (in the y direction) by an angle represented approximately by:

*This research was supported by NIH/NIAMS grant AR48292.

$$\Delta\theta(x, y) \equiv \frac{\partial}{\partial y} \int n(x, y, z) dz, \quad (2)$$

where $n(x, y, z)$ is refractive index distribution of the object. The aim of DEI is to recover the refraction angle $\Delta\theta$ and the attenuated intensity I_R at each image location (x, y) .

Herein, we derive an optimal maximum-likelihood (ML) estimator of these quantities from Poisson data. We find that, by chance, the ML solution is precisely the same as that of the original formulation of Chapman, *et al.* [1]. We then go on to determine the statistical properties—specifically, the mean, covariance, and signal-to-noise ratio (SNR)—of the ML-DEI solution.

Before we begin the ML derivation, let us first briefly review the quantities in DEI. DEI data consist of two images of the object, obtained at two rotational positions of the analyzer crystal (θ_L and θ_H), one on either side of the crystal system's angular reflectivity function (or *rocking curve*) $R(\theta)$. In the absence of noise, these images (denoted by I_L and I_H), are given by:

$$\bar{I}_L = E[I_L; \Theta] = I_R \left(R(\theta_L) + \frac{dR}{d\theta}(\theta_L) \Delta\theta \right), \quad (4)$$

$$\bar{I}_H = E[I_H; \Theta] = I_R \left(R(\theta_H) + \frac{dR}{d\theta}(\theta_H) \Delta\theta \right). \quad (5)$$

Here, $E[\cdot]$ is an expectation operator and we define Θ as a concatenation of the unknown parameters of interest, i.e., $\Theta = [\Delta\theta, I_R]^T$ where $[\cdot]^T$ is a transpose operator. Note that Eq (4) and (5) are strictly valid only if the object does not cause ultra-small-angle scattering, and if the magnitude of the refraction angle is small enough so that the rocking curve is well approximated by a first-order Taylor expansion.

If the imaging system is photon-limited, then the observations I_L and I_H can be represented as independent and Poisson distributed random variables, and the likelihood function is:

$$p(\mathbf{I}; \Theta) = \frac{\bar{I}_L^{I_L} e^{-\bar{I}_L}}{I_L!} \frac{\bar{I}_H^{I_H} e^{-\bar{I}_H}}{I_H!}, \quad (6)$$

where $\mathbf{I} = [I_L, I_H]^T$.

The ML estimator is obtained as:

$$\hat{\Theta}(\mathbf{I}) = \arg \max_{\Theta} [\ln p(\mathbf{I}; \Theta)]. \quad (7)$$

This maximization can readily be performed analytically by solving $\frac{\partial}{\partial \Theta} \ln p(\mathbf{I}; \Theta) = \mathbf{0}$ to obtain the following ML solution, which is identical to the standard DEI equations:

$$\hat{\Theta}(\mathbf{I}) = \begin{bmatrix} \Delta\hat{\theta} \\ \hat{I}_R \end{bmatrix} = \begin{bmatrix} \frac{I_H R(\theta_L) - I_L R(\theta_H)}{I_L \frac{dR}{d\theta}(\theta_H) - I_H \frac{dR}{d\theta}(\theta_L)} \\ \frac{I_L \frac{dR}{d\theta}(\theta_H) - I_H \frac{dR}{d\theta}(\theta_L)}{R(\theta_L) \frac{dR}{d\theta}(\theta_H) - R(\theta_H) \frac{dR}{d\theta}(\theta_L)} \end{bmatrix}. \quad (8)$$

Having derived the ML estimator now let us examine its mean, covariance and signal-to-noise ratio properties.

3. ESTIMATOR MEAN, COVARIANCE AND SIGNAL-TO-NOISE RATIO

Exact computation of the statistical properties of the ML estimator $\hat{\Theta}(\mathbf{I})$ produces a complex and unenlightening solution. Therefore, we apply an approximate method [6, 7] based on Taylor expansion of $\hat{\Theta}(\mathbf{I})$ around $\bar{\mathbf{I}}$ (the mean of \mathbf{I}) as follows:

$$\hat{\Theta}(\mathbf{I}) \equiv \hat{\Theta}(\bar{\mathbf{I}}) + \sum_{n \in \{L, H\}} \frac{\partial}{\partial I_n} \hat{\Theta}(\bar{\mathbf{I}}) (\bar{I}_n - I_n) + \frac{1}{2} \sum_{n \in \{L, H\}} \sum_{m \in \{L, H\}} \frac{\partial^2}{\partial I_n \partial I_m} \hat{\Theta}(\bar{\mathbf{I}}) (\bar{I}_n - I_n) (\bar{I}_m - I_m) + o(\mathbf{I}^3). \quad (9)$$

3.1. Conditions for unbiased estimation

We now show that the ML estimator is unbiased (produces results that are correct on average) if and only if two conditions are met. First, the noise variance must be equal to the signal (as is the case for Poisson noise); and second, the measurements must be taken at symmetric points of the rocking curve.

We begin our evaluation of the estimator mean by taking expectations of both sides of Eq (9) and utilizing the fact that observations I_L and I_H are independent. Now it is easy to show that Eq. (9) results in:

$$E[\hat{\Theta}(\mathbf{I})] \equiv \hat{\Theta}(\bar{\mathbf{I}}) + \frac{1}{2} \sum_{n \in \{L, H\}} \frac{\partial^2}{\partial I_n^2} \hat{\Theta}(\bar{\mathbf{I}}) \text{var}[I_n]. \quad (10)$$

The solution of Eq. (10) is presented in the Appendix, Eq. (A1), in the most general form using a well-known relation between the variance and mean of Poisson distributed data, i.e. $\text{var}[I_n] = E[I_n]$, $n \in \{L, H\}$.

Next, we assume that I_L and I_H are taken at symmetric points of the rocking curve (SPRC) so that $R(\theta_L) = R(\theta_H)$ and $\frac{d}{d\theta} R(\theta_L) = -\frac{d}{d\theta} R(\theta_H)$ where $\frac{d}{d\theta} R(\theta_L) > 0$. In the rest of the paper we refer to these assumptions as the SPRC conditions.

Now by utilizing the SPRC conditions it is easy to see that last the term in the numerator of Eq. (A1) will vanish and therefore:

$$E[\hat{\Theta}(\mathbf{I})] \equiv \hat{\Theta}(\bar{\mathbf{I}}), \quad (11)$$

and the estimator is unbiased.

Note that the refraction estimator is only unbiased if the noise variance equals the mean (i.e., the noise is Poisson-like).

3.2. Estimator covariance

Here we show that the estimates for refraction and attenuated intensity from Poisson distributed samples are uncorrelated only if measurements are taken at symmetric points of the rocking curve.

To calculate the covariance of the ML estimator $\hat{\Theta}(\mathbf{I})$ we use only the first two terms of the Taylor expansion in Eq.(9), which yields [6, 7]:

$$\text{cov}[\hat{\Theta}(\mathbf{I})] \equiv \nabla \hat{\Theta}(\bar{\mathbf{I}}) \text{cov}[\mathbf{I}] \nabla \hat{\Theta}(\bar{\mathbf{I}})^T. \quad (12)$$

As before, utilizing the fact that observations I_L and I_H are independent and Poisson distributed, one can obtain a solution for the most general case which is given in the Appendix in Eq. (A2). Here we proceeded by adopting the SPRC conditions, as we did for the mean. Since the last term in the numerator of each off-diagonal element is zero under the SPRC assumption, the solution becomes simply:

$$\text{cov}(\hat{\Theta}(\mathbf{I})) \equiv \begin{bmatrix} \frac{1}{2I_R} \left(\frac{R(\theta_L)}{\left[\frac{dR}{d\theta}(\theta_L) \right]^2} - \frac{(\Delta\theta)^2}{R(\theta_L)} \right) & 0 \\ 0 & \frac{I_R}{2R(\theta_L)} \end{bmatrix}. \quad (13)$$

So far we have shown that, under the SPRC assumptions and Poisson-like noise, the ML estimator $\hat{\Theta}(\mathbf{I})$ is unbiased and the absorption and refraction images are uncorrelated (off-diagonal elements in Eq. (13) are zero). However this is only true under the stated assumptions.

3.3. Signal-to-noise ratio

We define the SNR of each image as the ratio of the signal ($\Delta\theta$ or I_R), to the standard deviation of its estimate $[\text{var}(\Delta\hat{\theta})]^{1/2}$ or $[\text{var}(I_R)]^{1/2}$. Using Eq. (13), we obtain:

$$\text{SNR}(\hat{\Theta}(\mathbf{I})) \equiv \begin{bmatrix} \frac{|\Delta\theta| \frac{dR}{d\theta}(\theta_L) [2I_R R(\theta_L)]^{1/2}}{\left\{ R^2(\theta_L) - \Delta\theta^2 \left[\frac{dR}{d\theta}(\theta_L) \right]^2 \right\}^{1/2}} \\ [2I_R R(\theta_L)]^{1/2} \end{bmatrix} \quad (14)$$

Upon further analysis, this expression yields the following insights:

- The SNR of the attenuated intensity (\hat{I}_R) image is Poisson-like (it increases as the square root of the image intensity $I_R R(\theta_L)$).
- The SNR of the refraction-angle image $\Delta\hat{\theta}$ increases in an approximately linear fashion in terms of the following quantities:
 - the SNR of \hat{I}_R ;
 - the slope of the rocking curve $\frac{dR}{d\theta}(\theta_L)$; and
 - the absolute value of the refraction angle $|\Delta\theta|$.

Thus, SNR is improved by using a crystal diffraction order that produces a steep rocking curve, and using rocking curve points that are at the highest practical point on the rocking curve. The noise is signal-dependent in both the intensity and refraction-angle images; however, the SNR increases linearly with refraction signal, but only as the square root of the intensity signal. Finally, the refraction-image noise is dependent on the intensity signal, but the intensity-image noise does not depend on the refraction signal.

4. EXPERIMENTAL RESULTS

4.1. Monte Carlo simulation

Here we verify the results in Eqs. (11) and (13) by a Monte Carlo simulation. We simulated DEI data under the SPRC assumptions with 10^5 noise realizations.

First, we verified the estimator bias, which is predicted by Eq. (11) to be zero. In the simulation, we found the bias to be less than 0.01% over a wide range of object parameters.

Estimator variances obtained from the Monte Carlo simulation along with results obtained by the approximation in Eq. (13) are presented in Figure 2. There is excellent agreement between predicted performance and experimental results. Note that the variance of the I_R estimator does not depend on the refraction angle. However this is true only under the SPRC assumptions.

Equation (13) predicts that $\Delta\theta$ and I_R estimates are uncorrelated. In our simulation we found this to be true, with the correlation coefficient being less than 0.005.

The accuracy of the approximation increases with the beam intensity. This is expected since the Taylor expansion in Eq.(10) is strictly valid for a quadratic objective function [7] (e.g. log-likelihood of Gaussian distribution) and the Poisson distribution asymptotically approaches the Gaussian distribution as the beam intensity increases.

5. CONCLUSION

We have shown that the DEI method is a maximum-likelihood method, provided that the noise is Poisson-like and the data are acquired at symmetric points on the rocking curve. We have presented expressions for the mean, covariance, and SNR of DEI images, and verified them by Monte Carlo simulation. We find that DEI images are unbiased and uncorrelated if and only if the observations are Poisson-like and acquired at points of the rocking curve that have the same derivatives, namely $\frac{d}{d\theta} R(\theta_L) = -\frac{d}{d\theta} R(\theta_H)$.

In the future we plan to use presented results to evaluate various DEI reconstruction algorithms performance.

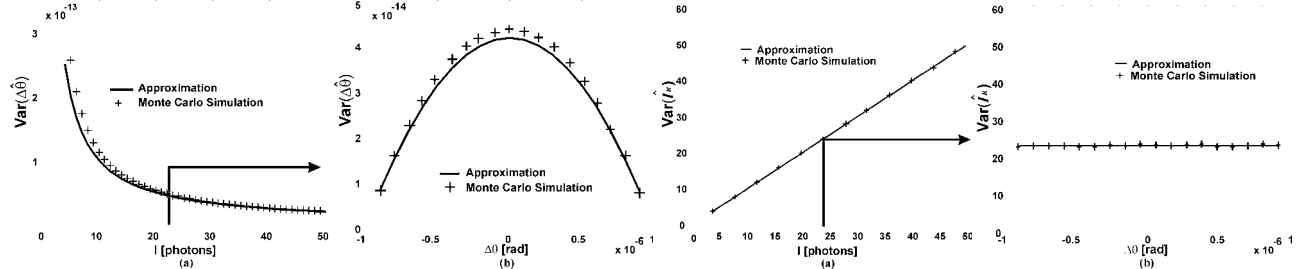


Fig. 2. Comparison of approximative expressions (Eq (13)) and Monte Carlo simulation. Variance of refraction angle estimator. (a) variance as a function of the number of photons emerging from the object for $\Delta\theta = 0$ rad; (b) variance as a function of refracted angle for $I_R = 24$ photons. Variance of transmitted beam intensity estimator, (c) variance as a function of intensity for $\Delta\theta = 0$ rad; (d) variance as a function of refracted angle for $I_R = 24$ photons. Note that agreement increases as the number of photons increases.

7. APPENDIX

From Eq. (12), using Eq (4) and (5), it can be shown that the DEI estimator mean is given in general by:

$$E[\hat{\boldsymbol{\theta}}(\mathbf{I})] \cong \hat{\boldsymbol{\theta}}(\bar{\mathbf{I}}) + \left[\frac{\begin{matrix} \left(R(\theta_H) + \frac{dR}{d\theta}(\theta_H)\Delta\theta \right) \left(R(\theta_L) + \frac{dR}{d\theta}(\theta_L)\Delta\theta \right) \left(R(\theta_L) \frac{dR}{d\theta}(\theta_H) - R(\theta_H) \frac{dR}{d\theta}(\theta_L) \right) \left(\frac{dR}{d\theta}(\theta_H) + \frac{dR}{d\theta}(\theta_L) \right) \\ I_R \left(R(\theta_L) \frac{dR}{d\theta}(\theta_H) - R(\theta_H) \frac{dR}{d\theta}(\theta_L) \right)^3 \\ 0 \end{matrix}}{\right]} \quad (\text{A1})$$

Similarly, from Eq. (14) using Eq (4) and (5) it can be shown that DEI estimator covariance is given in general by:

$$\text{cov}(\hat{\boldsymbol{\theta}}(\mathbf{I})) \cong \left[\begin{matrix} \frac{\left(R(\theta_H) + \frac{dR}{d\theta}(\theta_H)\Delta\theta \right) \left(R(\theta_L) + \frac{dR}{d\theta}(\theta_L)\Delta\theta \right) \left(R(\theta_H) + R(\theta_L) + \left(\frac{dR}{d\theta}(\theta_L) + \frac{dR}{d\theta}(\theta_H) \right) \Delta\theta \right)}{I_R \cdot \left(R(\theta_L) \frac{dR}{d\theta}(\theta_H) - R(\theta_H) \frac{dR}{d\theta}(\theta_L) \right)^2} & \frac{\left(R(\theta_H) + \frac{dR}{d\theta}(\theta_H)\Delta\theta \right) \left(R(\theta_L) + \frac{dR}{d\theta}(\theta_L)\Delta\theta \right) \left(\frac{dR}{d\theta}(\theta_H) + \frac{dR}{d\theta}(\theta_L) \right)}{\left(R(\theta_L) \frac{dR}{d\theta}(\theta_H) - R(\theta_H) \frac{dR}{d\theta}(\theta_L) \right)^2} \\ \frac{\left(R(\theta_H) + \frac{dR}{d\theta}(\theta_H)\Delta\theta \right) \left(R(\theta_L) + \frac{dR}{d\theta}(\theta_L)\Delta\theta \right) \left(\frac{dR}{d\theta}(\theta_H) + \frac{dR}{d\theta}(\theta_L) \right)}{\left(R(\theta_L) \frac{dR}{d\theta}(\theta_H) - R(\theta_H) \frac{dR}{d\theta}(\theta_L) \right)^2} & \frac{I_R \cdot \left(R(\theta_H) \frac{dR^2}{d\theta^2}(\theta_H) + R(\theta_L) \frac{dR^2}{d\theta^2}(\theta_L) + \left(\frac{dR}{d\theta}(\theta_H) \frac{dR^2}{d\theta^2}(\theta_L) + \frac{dR^2}{d\theta}(\theta_H) \frac{dR}{d\theta}(\theta_L) \right) \Delta\theta \right)}{\left(R(\theta_L) \frac{dR}{d\theta}(\theta_H) - R(\theta_H) \frac{dR}{d\theta}(\theta_L) \right)^2} \end{matrix} \right] \quad (\text{A2})$$

6. REFERENCES

- [1] D. Chapman *et al.* "Diffraction enhanced x-ray imaging", *Phys. Med. Biol.*, vol. 42, pp. 2015-2025, 1997.
- [2] M. O. Hasnah *et al.* "Diffraction enhanced imaging contrast mechanisms in breast cancer specimens", *Medical Physics*, vol. 29, no. 10, October 2002.
- [3] P. Suortti and W. Thomlinson, "Medical applications of synchrotron radiation", *Phys. Med. Biol.*, vol. 48, R1-R35, 2003.
- [4] E. D. Pisano *et al.*, "Human breast cancer specimens: diffraction enhanced imaging with histologic correlation-improved conspicuity of lesion detail compared with digital radiography", *Radiology*, 214, pp. 895-903, 2000.
- [5] A. Bravin, "Exploiting the x-ray refraction contrast with an analyzer: the state of the art," *J. Phys. D: Appl. Phys.* vol. 36, A24-A29, April 2003.
- [6] S. M. Kay "Fundamentals of statistical signal processing: Estimation theory", Prentice Hall: New Jersey, 1993.
- [7] J. A. Fessler "Mean and variance of implicitly defined biased estimators (such as penalized maximum likelihood): Application to tomography," *IEEE Trans. Image Proc.* vol. 5, no. 3, pp. 493-505, 1996.